

## Developing versus Nondeveloping Disturbances for Tropical Cyclone Formation. Part II: Western North Pacific\*

BING FU

*International Pacific Research Center, University of Hawaii at Manoa, Honolulu, Hawaii*

MELINDA S. PENG

*Marine Meteorology Division, Naval Research Laboratory, Monterey, California*

TIM LI

*International Pacific Research Center, and Department of Meteorology, University of Hawaii at Manoa, Honolulu, Hawaii*

DUANE E. STEVENS

*Department of Meteorology, University of Hawaii at Manoa, Honolulu, Hawaii*

(Manuscript received 9 September 2010, in final form 13 September 2011)

### ABSTRACT

Global daily reanalysis fields from the Navy Operational Global Atmospheric Prediction System (NOGAPS) are used to analyze Northern Hemisphere summertime (June–September) developing and nondeveloping disturbances for tropical cyclone (TC) formation from 2003 to 2008. This is Part II of the study focusing on the western North Pacific (WNP), following Part I for the North Atlantic (NATL) basin. Tropical cyclone genesis in the WNP shows different characteristics from that in the NATL in both large-scale environmental conditions and prestorm disturbances.

A box difference index (BDI) is used to identify parameters in differentiating between the developing and nondeveloping disturbances. In order of importance, they are 1) 800-hPa maximum relative vorticity, 2) rain rate, 3) vertically averaged horizontal shear, 4) vertically averaged divergence, 5) 925–400-hPa water vapor content, 6) SST, and 7) translational speed. The study indicates that dynamic variables are more important in TC genesis in the WNP, while in Part I of the study the thermodynamic variables are identified as more important in the NATL. The characteristic differences between the WNP and the NATL are compared.

### 1. Introduction

Many tropical disturbances occur each summer and fall, but only a small fraction of them develop into tropical cyclones (TCs). This study is the second part of a two-part investigation on developing and nondeveloping disturbances for TC formation in 2003–08 using global

daily analysis fields. In Peng et al. (2012, hereafter Part I) we analyzed developing and nondeveloping disturbances in the North Atlantic (NATL). In this Part II, we focus on the western North Pacific (WNP).

Limited observational data have been used in previous studies to contrast prestorm disturbances with nondeveloping disturbances. For example, using primarily rawinsonde data sources, McBride and Zehr (1981) found little difference in temperature and moisture fields between developing and nondeveloping cloud clusters in the WNP. The major difference was detected in flow characteristics between the developing and nondeveloping systems. An upper-level anticyclone, larger radial inflow, strong vertical upward motion, and a factor-of-2 greater tangential wind in the lower level distinguish

---

\* School of Ocean and Earth Science and Technology Contribution Number 8554 and International Pacific Research Center Contribution Number 853.

---

Corresponding author address: Tim Li, International Pacific Research Center, 1680 East-West Rd., POST 409B, Honolulu, HI 96822.  
E-mail: timli@hawaii.edu

the developing from nondeveloping systems. However, these developing cloud clusters included systems that had already reached tropical depression (TD) strength. In later studies, Lee (1989a,b) extended the dataset and showed that developing systems have stronger lower-level (below 850 hPa) radial inflow, greater upward motion inside 4° radius, up to two-times-greater cyclonic tangential wind speed extending from the disturbance center to 8° radius, and greater vertical wind shear opposite to the direction of the system movement. Zehr (1992) analyzed 50 prestorm disturbances and 22 nondeveloping disturbances during 1983/84 with conventional and satellite data. Weaker vertical wind shear, stronger low-level convergence, and sufficient low-level relative vorticity characterized tropical cyclogenesis. He viewed tropical cyclogenesis as a two-stage process. The first stage is marked by an increase in low-level relative vorticity, enhanced convection, and the formation of a low-level closed circulation center. Sea level pressure (SLP) and maximum sustained wind do not change much during the first stage. The second stage is characterized by a rapid SLP decrease and a significant increase of maximum winds consistent with gradient wind balance. By the end of this second stage, the system reaches the strength of a tropical storm (TS).

Dickinson and Molinari (2002) conducted a case study of tropical cyclogenesis in the western Pacific associated with a mixed Rossby–gravity (MRG) wave packet. A large-amplitude MRG wave packet was embedded in a convective region associated with active Madden–Julian oscillation (MJO) when it transitioned to a northwest-southeast-oriented tropical-depression-type wave train. Later, three TCs formed from the northwestward-moving wave train disturbances. Fu et al. (2007) analyzed tropical cyclogenesis events in the WNP during 2000/01 and found that 11 cyclogenesis events were associated with the TD-type wave train and about 40% of these wave trains originated from the MRG waves.

TC genesis over the WNP was analyzed by Chan and Kwok (1999) using the operational analyses of the Met Office global model for 1992/93. The analyses are divided into two groups depending on whether a particular analysis led to the prediction of a real genesis in the atmosphere. They found that 3 days prior to genesis, the low-level trades north of the pregenesis vortex begin to strengthen. One day later, an upper-level westerly trough and/or the tropical upper-tropospheric trough (TUTT) starts to approach the pregenesis cluster. While the low-level trades north of the cluster continue to intensify, a surge of southwesterly winds occurs to the south of the cluster. On the day before genesis, the southwesterlies become a dominant low-level feature. Camargo and Sobel (2004) analyzed western North Pacific tropical cyclone formation in an atmospheric general circulation

model. The model can simulate mean annual cyclone of storm number quite well. Their results show that environmental vertical shear peaks 2 days prior to tropical cyclone formation and then decreases. As they stated, this could indicate either a causal role of shear in limiting disturbance development or it could be consistent with a coincidental storm motion to regions of low shear. They also suggested dry lower troposphere is not favorable for tropical disturbance to amplify. Recently, Dunkerton et al. (2009) proposed a “critical layer” theory from a Lagrangian view to describe tropical cyclone genesis process. The critical layer is where the mean flow and the wave phase speed are similar, implying that a cutoff vortex will travel with the mean flow for some time and is the locus of wave–mean flow interaction and TC genesis. The wave serves as a “pouch” or sweet spot for cyclonic vortex development that protects the vortex from the usually hostile environment to allow upscale aggregation, convective moistening, and diabatic amplification.

This paper is Part II of an investigation on identifying different characteristics associated with developing and nondeveloping disturbances for TC formation in the WNP using 1°-resolution Navy Operational Global Atmospheric Prediction System (NOGAPS) daily reanalysis fields from 2003 to 2008. A detailed description of the data and methodology used to extract waves with a 3–8-day period representing the synoptic-scale precursor disturbance and a longer-than-20-day period representing the slowly varying environmental flow is given in Part I. There, 62 prestorm disturbances and 108 nondeveloping disturbances were identified during the Northern Hemisphere summertime in the NATL. It is well known that the WNP is the most active basin for TC activities in the world, with 36% of global TCs occurring in WNP, compared to 11% in the NATL (Gray 1968). Gray (1968) attributes this difference to different background climatology, disturbance type and source, and eddy–mean flow interactions.

This paper is organized as follows. In section 2, we compare the background climatology and disturbance characteristics between NATL and WNP. The mean composite differences between developing and nondeveloping disturbances in the WNP are presented in section 3. In section 4, we examine the variability within each group of the developing and nondeveloping disturbances and rank the key parameters based on a box difference index (BDI) analysis (Part I). A comparison of major genesis parameters in the NATL and the WNP is presented in section 5. The final section consists of a summary and discussion.

## 2. Background climatology in the WNP and NATL

To help identifying parameters controlling TC formations that may be different in NATL and WNP, we

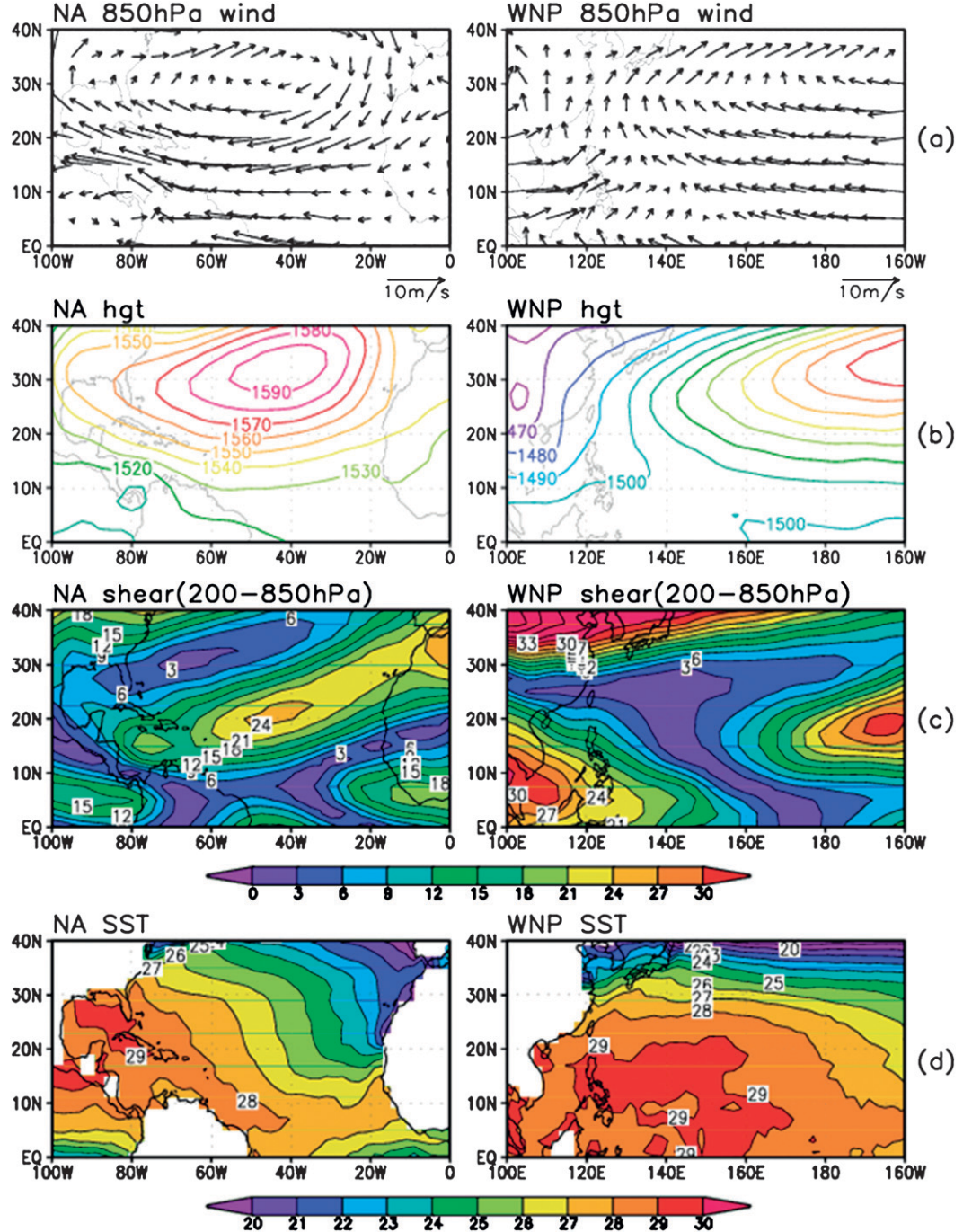


FIG. 1. Average (June–September) of monthly long term means in the (left) NATL and the (right) WNP from National Centers for Environmental Prediction–National Center for Atmospheric Research (NCEP–NCAR) reanalysis: (a) 850-hPa winds ( $\text{m s}^{-1}$ ); (b) 850-hPa geopotential heights (m); (c) Vertical shear speed between 200 hPa and 850 hPa ( $\text{m s}^{-1}$ ); and (d) SST ( $^{\circ}\text{C}$ ).

compare some major meteorological variables in the two basins. The June–September average 850-hPa winds, 850-hPa geopotential heights, vertical shear between 850 and 200 hPa, and SST fields are shown in Fig. 1. In the NATL (left panels), strong easterly winds (Fig. 1a)

dominate the lower troposphere south of the North Atlantic subtropical high (Fig. 1b). Vertical shear (speed) between 850 and 200 hPa shows a southwest–northeast-tilted sandwich pattern with a maximum value of  $24 \text{ m s}^{-1}$  located around  $20^{\circ}\text{N}, 45^{\circ}\text{W}$  (Fig. 1c).

The highest SST is located in the Gulf of Mexico, with a warm tongue extending southeastward to the West African coast (Fig. 1d). There are large east–west temperature gradients north of 15°N. Small temperature gradient over the tropical North Atlantic (south of 15°N) suggests that baroclinic instability may not play a major role in the growth of disturbances.

The right panels of Fig. 1 show the counterpart in the WNP. Unlike the NATL, where easterly trades and the subtropical high occupy the majority of tropical basin, the southwesterlies and associated western Pacific monsoon trough are important components of summer circulation in the WNP. The monsoon westerlies meet the trade easterlies, forming a zonal confluence zone that provides an ideal environment for wave energy accumulation (Webster and Chang 1988; Chang and Webster 1990, 1995; Kuo et al. 2001; Tam and Li 2006). Compared to the NATL, the distinct environmental flow features in the WNP include the monsoon trough, monsoon confluence zone (where westerlies meet easterlies), and monsoon shear line (with easterlies north of westerlies) (Ritchie and Holland 1999), which provide an ideal environmental condition for TC genesis.

The WNP has a long extending small vertical shear zone that overlaps the monsoon confluence zone and the monsoon shear line (Fig. 1c). In addition, the WNP has the largest warm pool in the world (Fig. 1d). While most of cyclogenesis events in the WNP occur over 29°C or warmer water, a significant number of TCs in the NATL form over a cooler water (<28°C) in the eastern basin. The western Pacific warm pool is also accompanied by large near-surface moisture content. All these favorable dynamic and thermodynamic environmental conditions make the WNP the most ideal region for TC genesis.

### 3. Composites

In addition to the environmental differences between WNP and NATL, disturbances that eventually evolved into a TC also show different characteristics between the two basins. While major precursor disturbances in the NATL are African easterly waves (AEWs), at least three types of low-level precursor disturbances are identified in the WNP by Fu et al. (2007). Their 2-yr (2000/01) statistics show that 18% of tropical storms in the WNP originated from a wave train generated because of Rossby wave energy dispersion of a preexisting TC (Li et al. 2003; Li and Fu 2006; Li et al. 2006), 21% from the Pacific easterly wave associated with extratropical forcing (Tam and Li 2006), and 32% from the TD-type synoptic wave train (Lau and Lau 1990) that is triggered by the instability of the summer mean flow in the presence of the convection–circulation feedback (Li 2006). The

TABLE 1. List of the number of developing and nondeveloping cases during the summer in the WNP from 2003–08.

	Developing					Nondeveloping				
	Jun	Jul	Aug	Sep	Tot	Jun	Jul	Aug	Sep	Tot
2003	1	2	5	3	11	5	3	5	3	16
2004	5	2	9	3	19	6	1	2	4	13
2005	0	6	5	6	17	3	3	5	1	12
2006	2	3	6	5	16	1	3	5	1	10
2007	0	3	5	6	14	5	4	5	6	20
2008	1	2	4	5	12	1	3	3	0	7
Tot	9	18	34	28	89	21	17	25	15	78

characteristics of developing and nondeveloping disturbances in the WNP are shown in this section, and are compared with results for NATL in Part I.

#### a. Geographic distribution of disturbances and translational speed

Using the same methodology and procedures described in Part I, 89 developing cases and 78 nondeveloping cases are identified in the WNP for the 2003–08 period. Table 1 lists the number of the developing and nondeveloping cases each year.

Figure 2a shows the displacement vectors for all the developing (from day −3 through day 0) and nondeveloping disturbances. The daily locations of the two groups are mixed and spread throughout the WNP with no preferred regions for either group. Figure 2b shows the averaged translational speed for the developing disturbances at day −3, −2, and −1 and nondeveloping disturbances. The averaged translational speed of all the developing cases is  $5.29 \text{ m s}^{-1}$ , which is slightly smaller than  $5.55 \text{ m s}^{-1}$  for the nondeveloping group. Even though the difference is small, a statistical test was conducted and the result shows that the difference between the translational speed of the developing disturbances at day −1 and that of the nondeveloping disturbances is significant at a 95% confidence level. This is consistent with the result in the NATL (Part I) that waves with a slower transitional speed are more likely to develop into a TC. However, the statistics of day −2 developers are virtually identical to that of nondevelopers.

#### b. Horizontal patterns

Following Part I, composites are made for day −3, −2, −1, and 0 for a  $20^\circ \times 20^\circ$  domain centered on the 850-hPa vorticity maximum, where day 0 denotes the genesis date according to the best-track data, and only one composite is made for the nondeveloping group. As in Part I, we do not display the day −2 composite, as they are generally similar to the day −1 composite. For each variable examined, three panels (day −3, −1, and 0) of the developing composites are compared with a single nondeveloping composite.

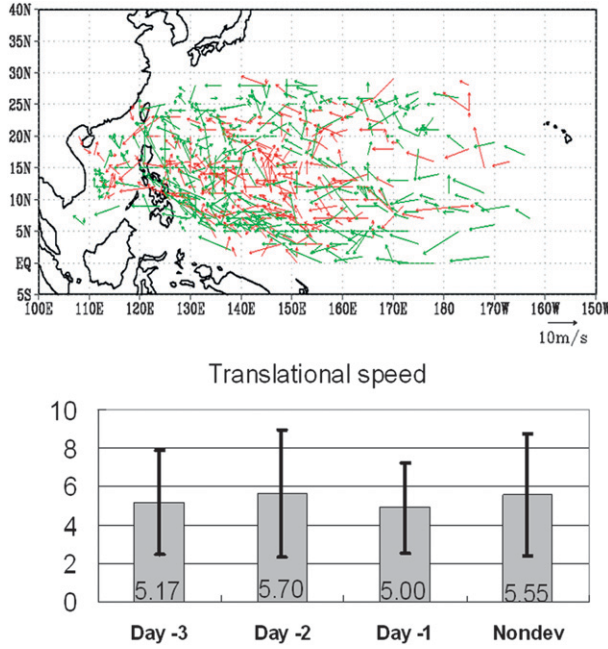


FIG. 2. (top) Daily displacement vectors of developing disturbances (red arrows) and nondeveloping disturbances (green arrows) in the WNP. (bottom) Average translational speed (bars) and corresponding standard deviation (whiskers). The value of average translational speed is marked at the bottom of each bar ( $\text{m s}^{-1}$ ).

Figure 3a shows the composites of 3–8-day filtered 850- (contours) and 500-hPa (shading) relative vorticity for the developing and nondeveloping cases. From day  $-3$  to 0, there is a gradual increase in the relative vorticity at both 850- and 500-hPa levels. Only the composite at day 0 shows clearly greater values than the nondeveloping composite, suggesting that cyclogenesis does not depend on the intensity of the precursor disturbance. This is the same as the finding in the NATL. However, the developing disturbances exhibit a more tightly compacted structure than the nondeveloping ones so that the radial vorticity gradient is greater for the developing waves. The relative vorticity centers are well lined up in the vertical for both groups, which is possibly a result of the convective parameterization in NOGAPS (Peng et al. 2004).

The Tropical Rainfall Measuring Mission (TRMM) Microwave Imager (TMI) SST composites are presented in Fig. 3b. The SST distributions for both groups are very similar, with a slightly tilted north–south gradient and a colder SST to the north of the nondeveloping waves. Note that the composite for developing disturbances are nosier than the nondeveloping ones. This is in part due to a smaller sample size for each time frame of the developing cases as they are divided into four subgroups of different dates. If a composite of all developing disturbances are

made—including the four time windows of day  $-3$ ,  $-2$ ,  $-1$ , and 0—the result is smoother (figure not shown). Similar characteristics also show up in the Atlantic but it is more distinct in the WNP because of its overall more uniform pattern. The domain-averaged SST at day  $-3$ ,  $-1$ , and 0 are  $29.29^\circ$ ,  $29.31^\circ$ , and  $29.28^\circ\text{C}$ , respectively. The difference among them is about 0.1% or less. Meanwhile, the domain-averaged SST for the nondeveloping group is  $29.13^\circ\text{C}$ . The SST difference between the developing and nondeveloping composites in the WNP is smaller than in the NATL. We will examine the importance of SST among other parameters later using BDI, which is introduced in Part I.

Figure 3c shows the relative humidity composites at 500 hPa. In general, higher relative humidity is located south of the disturbance center (Fig. 3b). This contrasts with the pattern in the NATL where the maximum of the relative humidity is closer to the center of the disturbance and the pattern is more symmetric with respect to the center. There is no obvious trend of the relative humidity change as disturbances develop. Overall, the relative humidity in the developing composite is about 5% higher than that in the nondeveloping composite.

The differences between the developing and nondeveloping disturbances are pronounced in the TMI precipitation composites (Fig. 4a). More intense precipitation is found in the developing group than in the nondeveloping groups. It is also evident that precipitation for developing disturbances increases as it develops further. Figure 4b depicts the magnitude of the environmental vertical shear between 850 and 200 hPa. Note that in the NATL, the environmental shear is taken between the 1000 and 600 hPa. The reason 850–200 hPa is chosen for WNP is obvious, as illustrated by the vertical profile of the zonal wind in the next section (Fig. 5). A large difference between the developing and nondeveloping cases appears in both the pattern and magnitude. In contrast to the NATL (see Part I) where a smaller vertical shear is observed for developing disturbances, the WNP composites show that the developing disturbances propagate into an environment with a slightly greater vertical shear, particularly to the south of the disturbance center. The domain-averaged magnitude of the vertical shear speed is  $11.33 \text{ m s}^{-1}$  for the developing cases at day  $-1$ , in comparison to  $11.14 \text{ m s}^{-1}$  for the nondeveloping cases. Therefore, for the magnitude of vertical shear, there is no significant difference between the developing and nondeveloping disturbances. Note that the vertical shear patterns for the developing disturbances have a large north–south gradient, with the largest shear in the southwest of the domain. By contrast, the nondeveloping group has a smoother horizontal distribution. The composites of 20-day low-pass filtered 850-hPa divergence fields are

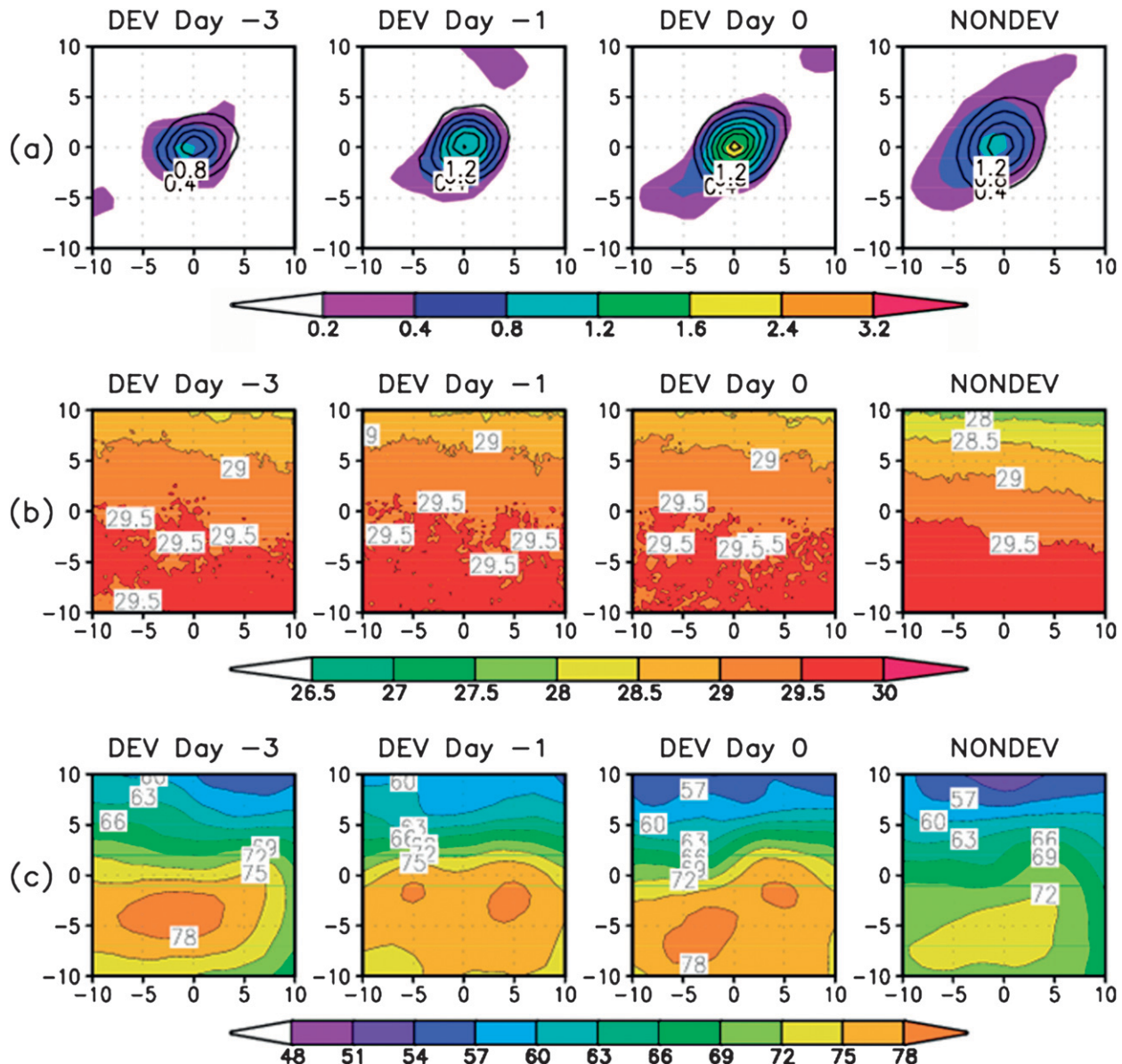


FIG. 3. Composite fields for developing and nondeveloping disturbances in the WNP. (a) 3–8-day filtered relative vorticity at 850 hPa (contours, interval = 0.4) and 500 hPa (shading) ( $10^{-5} \text{ s}^{-1}$ ), (b) SST ( $^{\circ}\text{C}$ ), and (c) relative humidity (%) at 500 hPa. For all the composite fields, the horizontal/vertical axis measures relative longitudinal/latitudinal distance in degrees from the center.

shown in Fig. 4c. All composite panels for the developing disturbances exhibit greater low-level convergences than for the nondeveloping disturbances, similar to what is observed in NATL. Figure 4d depicts the 850-hPa horizontal shear ( $\partial u / \partial y$ ). A distinct strong shear zone near the center of the disturbance is associated with developing disturbances. Unlike that in the NATL, this parameter turns out to be one of the most important dynamic parameters for TC genesis in the WNP, as will be revealed later by the BDI calculation in section 4.

#### c. Vertical profiles of the wind and humidity

The vertical profile of the domain-averaged zonal wind is depicted in Fig. 5. This vertical profile with easterly shear within the boundary layer below 850 hPa and westerly shear above is different from the profile observed in the NATL, where there is westerly shear below 600 hPa and easterly shear above. A shear between 850 and 200 hPa appears to be a reasonable choice to define the environmental wind conditions here (shown in Fig. 4b). In contrast to a decreasing trend of

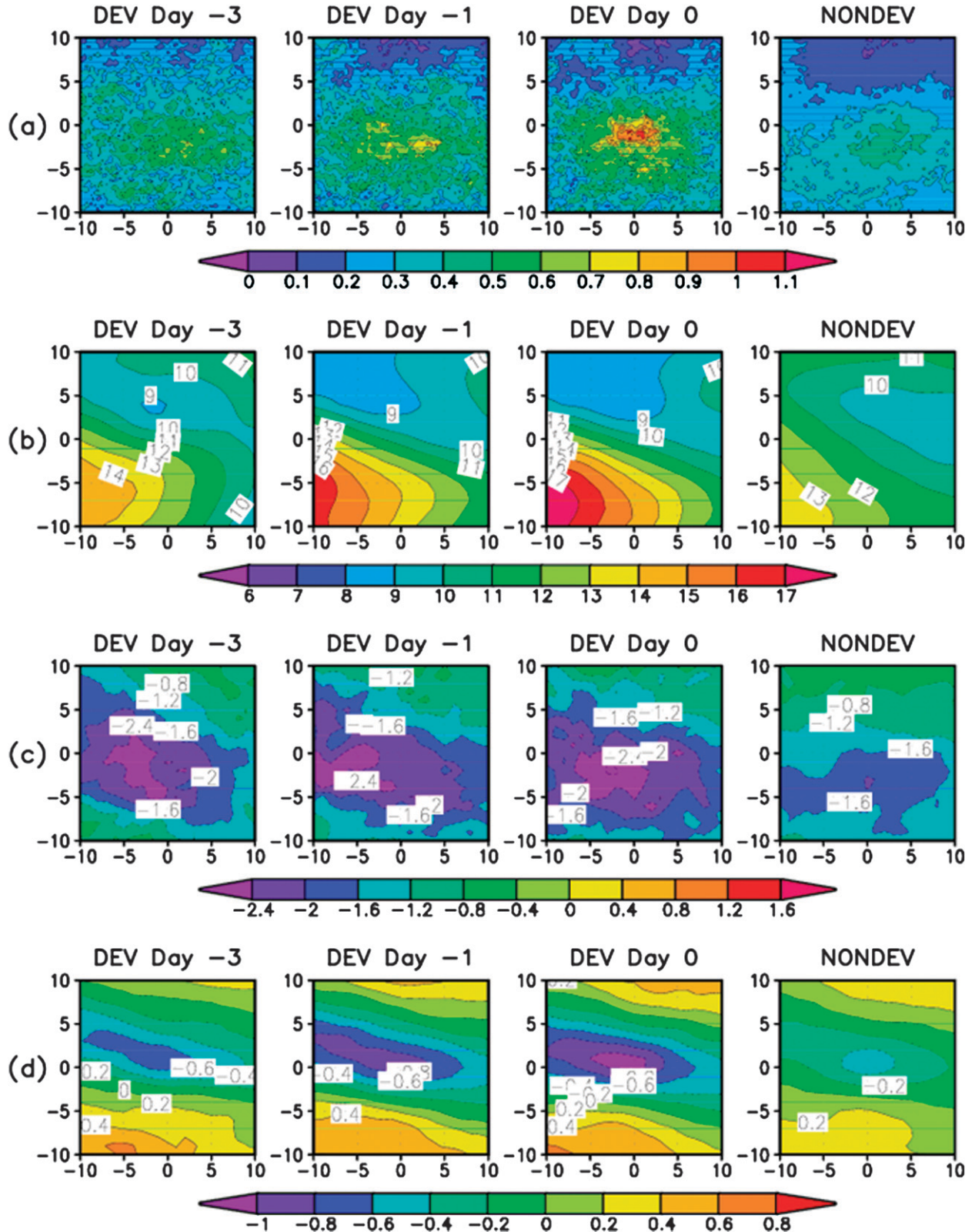


FIG. 4. Composite fields for developing and nondeveloping disturbances in the WNP. (a) Rain rate ( $\text{mm hr}^{-1}$ ), (b) speed of 20-day low-pass filtered wind shear between 200 hPa and 850 hPa ( $\text{m s}^{-1}$ ), (c) 20-day low-pass filtered 850-hPa divergence ( $10^{-6} \text{ s}^{-1}$ ), and (d) 20-day low-pass filtered 850-hPa  $\partial u / \partial y$  ( $10^{-5} \text{ s}^{-1}$ ). For all the composite fields, the horizontal/vertical axis measures relative longitudinal/latitudinal distance in degrees from the center.

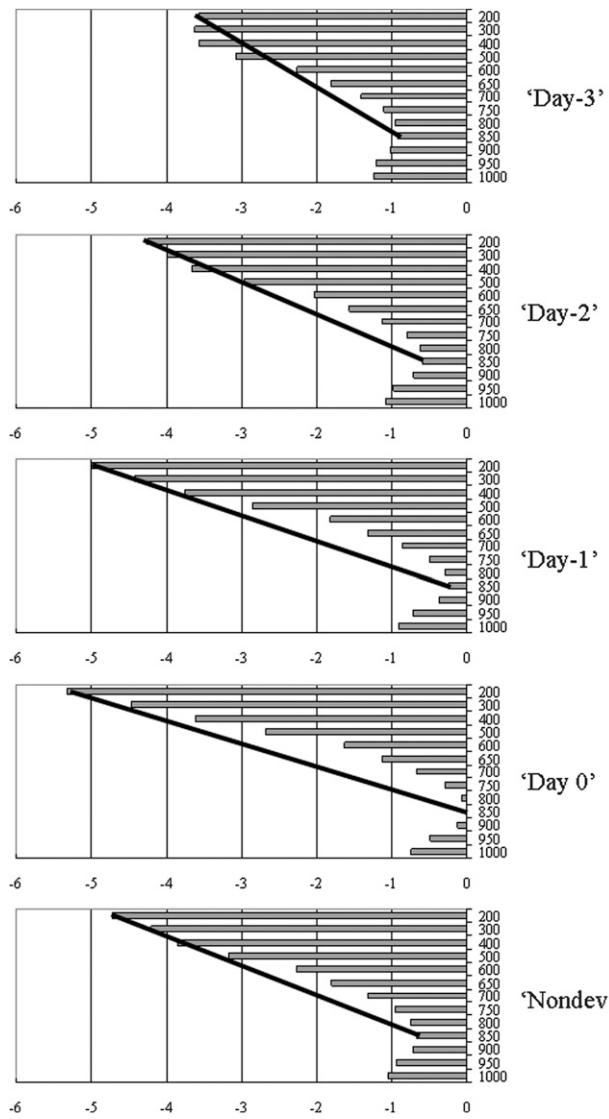


FIG. 5. Vertical profiles of  $10^\circ \times 10^\circ$  domain-averaged composites of 20-day low-pass filtered zonal wind for developing and nondeveloping disturbances in the WNP ( $\text{m s}^{-1}$ ).

the shear in the NATL as TC develops, the vertical shear of the zonal wind between 850 and 200 hPa in the WNP actually exhibits an increasing trend from day  $-3$  to  $0$  for the developing cases. Its magnitude is about  $2.64 \text{ m s}^{-1}$  at day  $-3$ , increasing to  $4.76 \text{ m s}^{-1}$  at day  $-1$  and  $5.32 \text{ m s}^{-1}$  at day  $0$ . The average shear magnitude is  $4.06 \text{ m s}^{-1}$  for all the nondeveloping cases. However, a statistical test shows that the vertical shear difference between the developing and nondeveloping disturbance groups is not significant because of the large variation within each group. This is also revealed by the BDI computation later.

The vertical profiles of large-scale, domain-averaged horizontal shear of the zonal wind ( $\partial u / \partial y$ ) are shown in

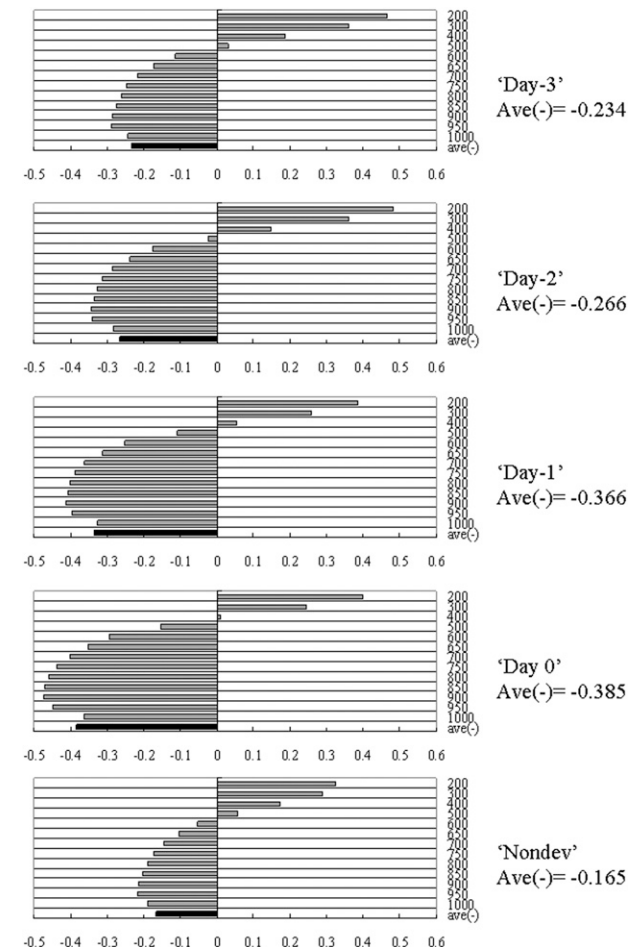


FIG. 6. Vertical profiles of  $20^\circ \times 10^\circ$  domain-averaged composites of 20-day low-pass filtered  $\partial u / \partial y$  ( $10^{-5} \text{ s}^{-1}$ ) for developing and nondeveloping disturbances in the WNP. The black bar in each of panel represents vertical average of negative bars (averaged value is marked to the right of panel) at lower levels.

Fig. 6. Though the magnitude of the horizontal wind shear is small, a distinct difference between the developing and nondeveloping disturbances is evident with the cyclonic shear of the developing disturbances nearly twice that of the nondeveloping disturbances. The developing disturbances also have a lightly deeper layer of this cyclonic shear. Accompanying the greater cyclonic shear in the lower troposphere, a greater anticyclonic shear appears in the upper troposphere in the developing disturbance composites. The deeper and larger cyclonic shear of the developing disturbances could be related to large-scale circulation pattern like a stronger monsoon gyre, favoring TC development as proposed by Ritchie and Holland (1999).

Figure 7 depicts the vertical distribution of the divergence. The vertical distributions of the divergence for developing and nondeveloping disturbances look

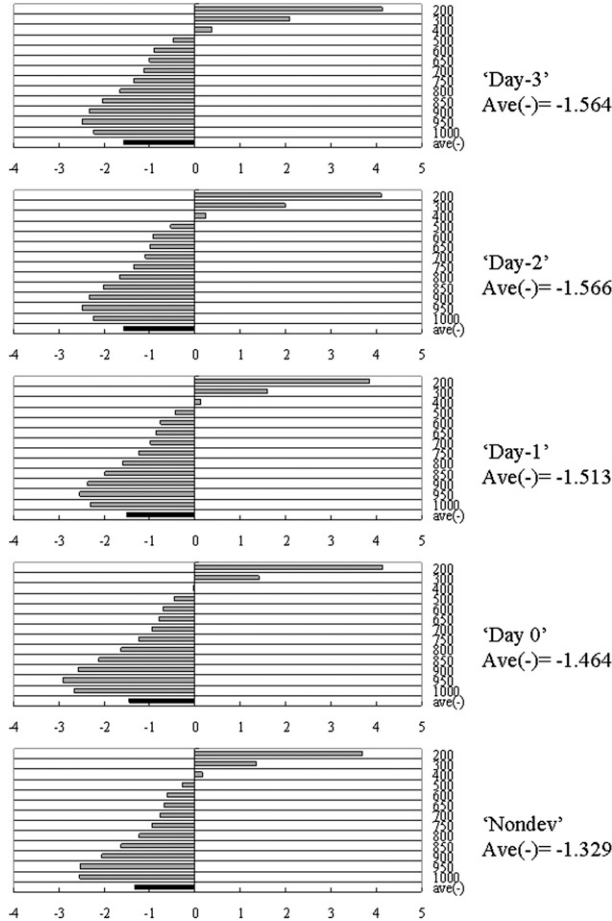


FIG. 7. Vertical profiles of  $10^\circ \times 10^\circ$  domain-averaged composites of 20-day low-pass filtered divergence ( $10^{-6} \text{ s}^{-1}$ ) for developing and nondeveloping disturbances in the WNP. The black bar in each of panel represents vertical average of negative bars (averaged value is marked to the right of panel) at lower levels.

quite similar. While checking the magnitude of the divergence at each level, we find that developing disturbances have stronger convergence. This is verified by a significant test shown in later sections. Compared to the NATL, developing and nondeveloping groups both have a thicker layer of low-level convergence. This is related to the large monsoon gyre in the WNP. The convergence field has a significant contribution in TC development, which is shown by the BDI computation in the next section.

Comparison of vertical profiles of specific humidity averaged within two horizontal domains with different sizes shows generally a similar finding to that in the NATL. The developing disturbances possess greater specific humidity than the nondeveloping disturbances at each vertical level (Figs. 8a,b). The difference between the developing and nondeveloping disturbances is more distinguishable in the lower troposphere. The largest

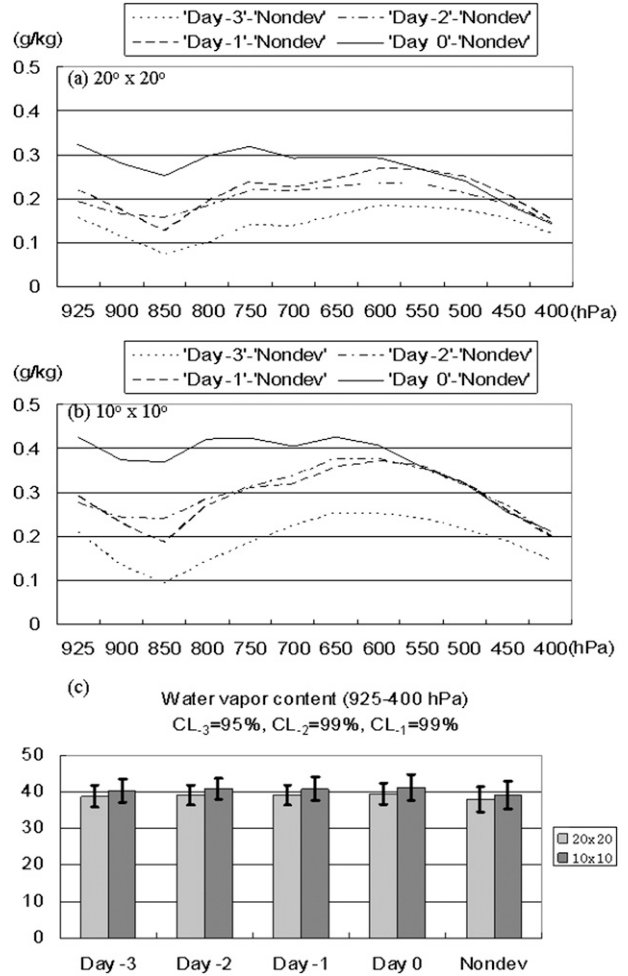


FIG. 8. Difference of domain-averaged specific humidity between the developing and nondeveloping disturbances at different vertical levels (a) in a  $20^\circ \times 20^\circ$  domain and (b) in a  $10^\circ \times 10^\circ$  domain; and (c) domain-averaged ( $20^\circ \times 20^\circ$  in light gray,  $10^\circ \times 10^\circ$  in dark gray) composite of water vapor content (925–400 hPa) (kg). CL<sub>-3</sub>, CL<sub>-2</sub>, and CL<sub>-1</sub> denote the comparison of developing disturbances at day -3, -2, and -1 with nondeveloping disturbances is statistically significant at confidence level 95%, 99%, and 99%.

difference occurs at day 0 and the smallest difference occurs at day -3, whereas the differences between day -2 and -1 are quite similar throughout the troposphere. The 925–400-hPa water vapor content shows a gradually increasing trend from day -3 to 0 for the developing disturbances (Fig. 8c). For all 4 days, from day -3 to 0, the water vapor content is greater than that of the nondeveloping composite. The difference for each of the developing days is statistically significant (with a *t* test) at a 95% or 99% confidence level.

In summary, significant differences exist between the developing and nondeveloping disturbances. The developing disturbances are characterized by slower

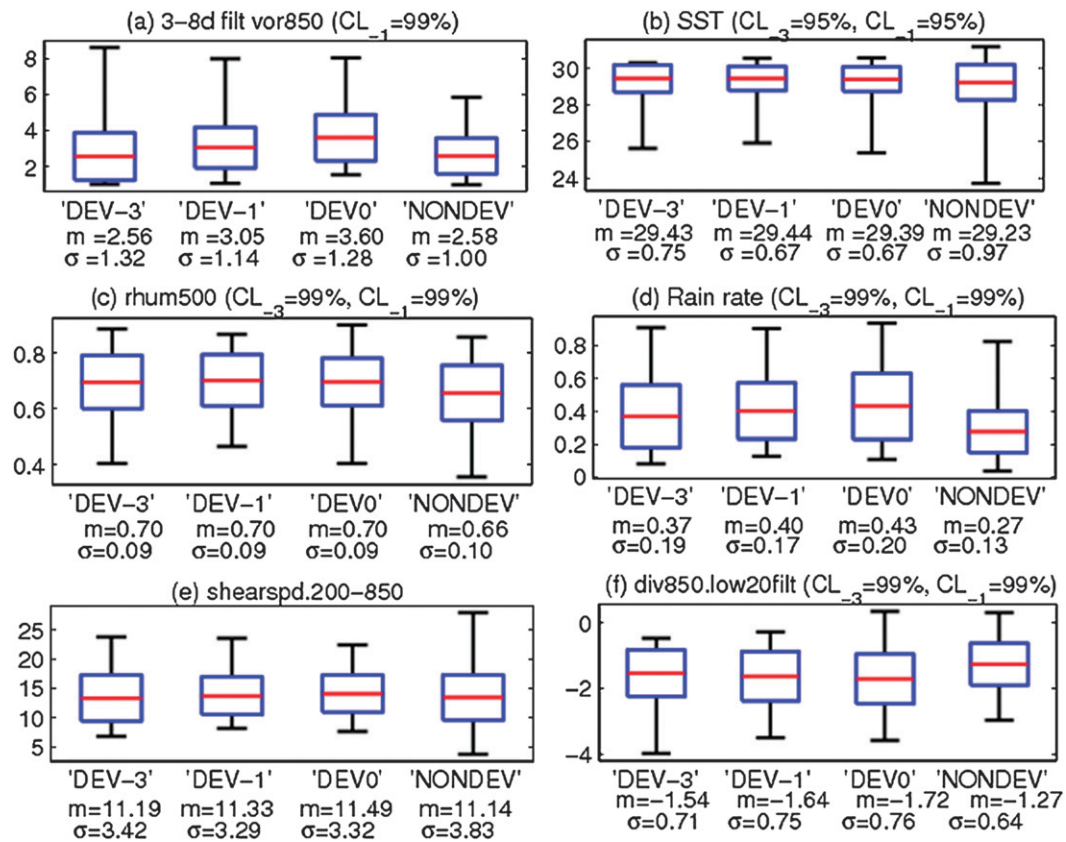


FIG. 9. Box-and-whiskers figures for (a) maximum 3–8-day filtered 850-hPa relative vorticity ( $10^{-5} \text{ s}^{-1}$ ) and  $20^\circ \times 20^\circ$  box averaged; (b) SST ( $^{\circ}\text{C}$ ); (c) 500-hPa relative humidity (%); (d) rain rate ( $\text{mm hr}^{-1}$ ); (e) 20-day low-pass filtered vertical wind shear speed between 200 hPa and 850 hPa ( $\text{m s}^{-1}$ ); and (f) 20-day low-pass filtered 850-hPa divergence ( $10^{-6} \text{ s}^{-1}$ ). Mean is denoted by  $m$  (red line), sigma denotes the standard deviation. A blue box depicts the variation between  $m - \sigma$  and  $m + \sigma$ . Whiskers represent the minimum and maximum of the samples.  $CL_{-3}$  ( $CL_{-1}$ ) denotes that the difference between the developing disturbances at day  $-3$  (day  $-1$ ) and the nondeveloping disturbances is statistically significant at a confidence level of 95% or 99%.

translational speed, warmer SST, larger convergence, greater horizontal cyclonic shear, and higher moisture content. Note that the nondeveloping disturbances possess smaller vertical shear, which is in contrast to conventional wisdom, but the difference is not significant.

#### 4. Variability of samples within each group and BDI

As introduced in Part I, the BDI takes into account both the mean and variability differences and thus is a useful index to separate the developing disturbances from the nondeveloping ones. For each key variable shown in Figs. 3 and 4, we plotted the corresponding box-and-whiskers figures to illustrate their spread within each of the developing and nondeveloping groups (Fig. 9). The advantage of the box-and-whiskers plot is that it shows the mean, standard deviation, and extremities in a single figure. It is worth noting that the vorticity and

SST plots show a different feature in the extremities. For vorticity, the means are all far away from the maximum and closer to the minimum. This is in part due to the thresholds we impose in selecting the disturbances for the developing and nondeveloping disturbances. The opposite holds for the SST plots, in which the means are far away from the minimum and closer to the maximum. The small difference between the mean and upper bound of SST is attributed to the fact that the averaged SST in the WNP is quite high and there are dynamic and thermodynamic regulating mechanisms in the warm pool (Ramanathan and Collins 1991; Wallace 1992; Sun and Liu 1996; Li et al. 2000). In the lower bound, it is interesting to note that for extreme cases, cyclogenesis may occur in cooler water with the domain-averaged SST below  $26^{\circ}\text{C}$ .

The relative humidity at 500 hPa, rain rate, and large-scale convergence at 850 hPa for the developing disturbances all show a larger mean value compared to that

TABLE 2. Different characteristics between developing cases and nondeveloping cases in the WNP.

	Developing	Nondeveloping
Translational speed	Slow	Fast
Relative vorticity	Large	Small
SST	High	Low
500-hPa relative humidity	High	Low
Rainfall	Intense	Weak
925–400-hPa water vapor content	Large	Small
Background convergence	Strong	Weak
Cyclonic horizontal shear	Strong	Weak

of the nondeveloping disturbances. A statistical test confirms that the difference between developing disturbances at any day (day  $-3$ ,  $-2$ ,  $-1$ , and  $0$ ) and nondeveloping disturbances is significant at a 99% confidence level. Whereas the domain-averaged relative humidity at 500 hPa remains steady from day  $-3$  to  $0$ , the mean precipitation and convergence show an increasing trend as the genesis date approaches. The mean of the vertical wind shear between 200 and 850 hPa increases slightly in pregenesis disturbances, but the difference of it with the nondeveloping cases does not pass the statistical significance test. Both the SST and the vertical wind shear show large variability in the nondeveloping groups. The result supports the notion that TC formation is determined by the collective effects of multiple (dynamic and thermodynamic) factors and that the main controlling factors for cyclogenesis might differ in different basins.

To summarize, in general, the developing disturbances in the WNP have the following characteristics that distinguish them from the nondeveloping disturbances, slower translational speed, greater synoptic relative vorticity, higher SST, higher relative humidity at 500 hPa, more intense rainfall, stronger background 850-hPa convergence, large cyclonic shear, and greater water vapor content. These characteristics are listed in Table 2.

Following the procedures in Part I, we calculated the BDIs for key parameters that were well known and relevant for TC formation and rank them according to the BDI. Table 3 shows the sorted list of important genesis parameters for the WNP. By comparing the BDI values for the key variables, we found that the relative vorticity at 800 hPa is the most important parameter to differentiate the developing and nondeveloping disturbances in the WNP. The second most important parameter is the rain rate. The vertically averaged horizontal shear and divergence ranks third and fourth, respectively, with nearly the same value. The last group of importance contains SST and translational speed. The vertical wind shear does not appear in the list, as its BDI value is

TABLE 3. Ranks of key genesis parameters in the WNP and their corresponding BDI values (magnitude and sign).

	BDI		
Variable name	Sign	Magnitude	
800-hPa max relative vorticity	+	0.46	
Rain rate ( $20^\circ \times 20^\circ$ )	+	0.42	
Vertically averaged $\partial u / \partial y$ ( $20^\circ \times 10^\circ$ )	-	0.39	
Vertically averaged divergence ( $10^\circ \times 10^\circ$ )	-	0.38	
925–400-hPa water vapor content ( $10^\circ \times 10^\circ$ )	+	0.24	
SST ( $20^\circ \times 20^\circ$ )	+	0.13	
Translational speed	-	0.06	

negligible. Based on this table, it is clear that dynamic variables (and rain rate) are more crucial than the thermodynamic variables for tropical cyclogenesis in the WNP.

## 5. Comparison of the genesis-controlling parameters between WNP and NATL

Tropical disturbances in the NATL and the WNP share many similar characteristics even though they reside in different environments. In the NATL (Part I), we found that the developing disturbances differ from the nondeveloping disturbances for TC formation with the following marked characteristics, in the order of importance determined by BDI: 1) 925–400-hPa water vapor content, 2) rain rate, 3) SST, 4) 700-hPa maximum relative vorticity, 5) 1000–600-hPa vertical shear, 6) translational speed, and 7) vertically averaged horizontal shear. The list indicates that the thermodynamic effect is more important than the dynamic effect in the NATL.

Similar characteristics associated with developing disturbances are also found in the WNP, except that the rank of importance is quite different, as in the following: 1) 800-hPa maximum relative vorticity, 2) rain rate, 3) vertically averaged horizontal shear, 4) vertically averaged divergence, 5) 925–400-hPa water vapor content, 6) SST, and 7) translational speed. The vertical wind shear in the WNP is not in the list, as its BDI number is very small.

As day  $0$  is the time when the prestorm disturbance has reached the critical amplitude, different characteristics between the two basins at that time might reflect different genesis processes. Note that a large difference appears in the low-level, large-scale convergence field that may distinguish the cyclogenesis processes between the NATL and WNP. In the WNP,

TABLE 4. Comparison of top four key genesis parameters in the NATL and the WNP. The “T” denotes the thermodynamic factor and “D” denotes the dynamic factor.

BDI rank	Basin	
	NATL	WNP
1	T	D
2	T	T
3	T	D
4	D	D

the large-scale convergence associated with the monsoon gyre may organize smaller-scale eddies or vertical hot towers to merge, or that wave energy may accumulate in a critical location (Kuo et al. 2001; Li et al. 2003; Tam and Li 2006). In the NATL, the large-scale convergence does not stand out as a key controlling parameter, while the vertical shear is important among the dynamic parameters. We speculate that the large-scale convergence and large horizontal shear in the WNP can offset the detrimental effort of a larger shear observed when we are following developing waves. However, one should also be aware that strong low-level convergence and large cyclonic shear do not always coexist with strong vertical shear (Fig. 1). This remains to be verified using a more idealized framework and controlled environment in the future.

Previous studies (e.g., Gray 1968; Emanuel and Nolan 2004) proposed a set of universal cyclogenesis parameters for the entire tropical oceans. Given the distinctive mean circulation and disturbance characteristics, it is likely that the relative importance of dynamic and thermodynamic parameters differs between the NATL and WNP. Table 4 compares the top four parameters that are most important for TC formation in the NATL and the WNP based on our BDI calculations following individual disturbances. It is interesting to note that while dynamic parameters appear to dominate TC formation in the WNP, it is the thermodynamic factors that play a major role in determining whether or not a disturbance will develop in the NATL.

## 6. Summary and discussion

Six years (2003–08) of NOGAPS daily analysis fields and TMI satellite data are used to analyze the characteristics of developing and nondeveloping disturbances in the Lagrangian framework over the North Atlantic (Part I) and the western North Pacific (Part II).

TC genesis in the WNP differs from that in the NATL in both the large-scale background environmental conditions and disturbance types and sources. The WNP exhibits a pronounced monsoon flow, which

differs markedly from the dominant easterly trade regime in the NATL. This monsoon circulation contributes to a more pronounced large-scale convergence and horizontal shear associated with developing disturbances for TC formation. The WNP is characterized by a rather uniform SST zonally in the warm-pool region (with a small north-south gradient) favorable for TC genesis, and therefore, the SST difference between developing and nondeveloping disturbances is not significant. In the Atlantic, the SST exhibits a strong east-west gradient along the direction where waves propagate, and the SST difference between the developing and nondeveloping groups is significant.

While most of the synoptic disturbances in the NATL are AEWs, prestorm disturbances in the WNP originate from various sources, including Rossby wave trains induced by tropical cyclone energy dispersion, easterly waves associated with extratropical forcing, and TD-type synoptic wave trains/mixed Rossby–gravity waves (Fu et al. 2007).

An index (BDI) is introduced to reveal the relative importance of various parameters in TC genesis. The BDI takes into account both the mean and standard deviation of the developing and nondeveloping groups. Based on the BDI value, the major genesis parameters are ranked for both the WNP and NATL basins (see section 5). Our results show that, in contrast to the NATL where the thermodynamic/moisture factors play dominant roles, dynamic factors are more important in controlling the TC formation in the WNP. Earlier studies by McBride and Zehr (1981) and Lee (1989a,b) found that the thermodynamic variables (temperature and moisture) have little difference between developing and nondeveloping disturbances. Meanwhile, dynamic flow characteristics (tangential flow and boundary layer inflow) are distinctive between the two groups. Our findings are consistent with theirs.

Camargo et al. (2007) investigated the environmental factors contributing to TC activities under ENSO influence using NCEP monthly reanalysis in the period of 1950–2004. They computed the genesis index developed by Emanuel and Nolan (2004) in a latitude trip from 60°S to 60°N. Their results indicate that specific factors have more influence in different regions. In the El Niño year, relative humidity and vertical shear are important for reduction in genesis in the Atlantic basin, while relative humidity and vorticity are important for the eastward shift in the genesis location in the WNP. Our results, following the disturbances in Lagrangian framework, indicate that vertical shear parameter is not as important as other parameters in the WNP, but is important in the NATL. Tropical regions contain large variability from place to place so that different characteristics can be

found when viewing a broader region with a longer time scale than by looking at individual disturbances. This is reflected by the different characteristics shown for our investigation when the NATL is divided into two parts (Part I).

The results above indicate that cyclogenesis processes exhibit marked regional contrasts and it is necessary to differentiate them in the cyclogenesis forecast for both weather and climate. The application of our study should be limited to identifying the potential of TC formulation for individual disturbances only. We plan to extend the current BDI analysis to the tropical eastern Pacific, Indian Ocean, and southwestern Pacific basins in future studies.

One of the most challenging tasks in numerical weather prediction is the capability of predicting TC genesis. Recent studies show that numerical models with a grid size near 10 km and explicit cloud-resolving schemes are required to simulate the evolution of TC precursors and predict the occurrence of TC genesis events (Jin et al. 2008). Based on different factors we found in controlling the TC genesis events in different basins, we propose that the numerical modeling effort on TC genesis should focus on physical parameterization in the NATL and focus on numerical schemes and model resolution in the WNP. The results from this study also inspire us to construct a nonlinear logistic regression model (with the BDI-determined genesis parameters for each basin) to forecast TC genesis at a 1–3-day lead time that is applied to individual disturbances in operational analysis or forecast fields. Preliminary results are encouraging and a detailed report is in preparation.

Even though similar parameters are identified for TC genesis, the main difference between our study and others is that our analysis follows individual disturbances, while most other studies focus on TC genesis over broader regions.

**Acknowledgments.** We thank Drs. Thorncroft and Dunkerton and another anonymous reviewer for their valuable comments and constructive suggestions. We also thank Ms. May Izumi for her editorial service. This study was supported by ONR Grants N000140810256 and N000141010774, NRL Subcontract N00173-06-1-G031, and the International Pacific Research Center, which is sponsored by the Japan Agency for Marine-Earth Science and Technology (JAMSTEC), NASA (Grant NNX07AG53G), and NOAA (Grant NA17RJ1230).

#### REFERENCES

- Camargo, S. J., and S. H. Sobel, 2004: Formation of tropical storms in an atmospheric general circulation model. *Tellus*, **56A**, 56–67.
- , K. A. Emanuel, and A. H. Sobel, 2007: Use of a genesis potential index to diagnose ENSO effects on tropical cyclone genesis. *J. Climate*, **20**, 4819–4834.
- Chan, J. C. L., and R. H. F. Kwok, 1999: Tropical cyclone genesis in a global numerical weather prediction model. *Mon. Wea. Rev.*, **127**, 611–624.
- Chang, H.-R., and P. J. Webster, 1990: Energy accumulation and emanation at low latitudes. Part II: Nonlinear response to strong episodic equatorial forcing. *J. Atmos. Sci.*, **47**, 2624–2644.
- , and —, 1995: Energy accumulation and emanation at low latitudes. Part III: Forward and backward accumulation. *J. Atmos. Sci.*, **52**, 2384–2403.
- Dickinson, M., and J. Molinari, 2002: Mixed Rossby–gravity waves and western Pacific tropical cyclogenesis. Part I: Synoptic evolution. *J. Atmos. Sci.*, **59**, 2183–2196.
- Dunkerton, T. J., M. T. Montgomery, and Z. Wang, 2009: Tropical cyclogenesis in a tropical wave critical layer: Easterly waves. *Atmos. Chem. Phys.*, **9**, 5587–5646.
- Emanuel, K. A., and D. Nolan, 2004: Tropical cyclone activity and the global climate system. Preprints, 26th Conf. on Hurricanes and Tropical Meteorology, Miami, FL, Amer. Meteor. Soc., 240–241. [Available online at [http://ams.confex.com/ams/26HURR/techprogram/paper\\_75463.htm](http://ams.confex.com/ams/26HURR/techprogram/paper_75463.htm).]
- Fu, B., T. Li, M. S. Peng, and F. Weng, 2007: Analysis of tropical cyclogenesis in the western North Pacific for 2000 and 2001. *Wea. Forecasting*, **22**, 763–780.
- Gray, W. M., 1968: A global view of the origin of tropical disturbances and storms. *Mon. Wea. Rev.*, **96**, 669–700.
- Jin, Y., M. S. Peng, and H. Jin, 2008: Simulating the formation of Hurricane Katrina (2005). *Geophys. Res. Lett.*, **35**, L11802, doi:10.1029/2008GL033168.
- Kuo, H.-C., J.-H. Chen, R. T. Williams, and C.-P. Chang, 2001: Rossby waves in zonally opposing mean flow: Behavior in northwest Pacific summer monsoon. *J. Atmos. Sci.*, **58**, 1035–1050.
- Lau, K. H., and N. C. Lau, 1990: Observed structure and propagation characteristics of tropical summertime synoptic scale disturbances. *Mon. Wea. Rev.*, **118**, 1888–1913.
- Lee, C. S., 1989a: Observational analysis of tropical cyclogenesis in the western North Pacific. Part I: Structural evolution of cloud clusters. *J. Atmos. Sci.*, **46**, 2580–2598.
- , 1989b: Observational analysis of tropical cyclogenesis in the western North Pacific. Part II: Budget analysis. *J. Atmos. Sci.*, **46**, 2599–2616.
- Li, T., 2006: Origin of the summertime synoptic-scale wave train in the western North Pacific. *J. Atmos. Sci.*, **63**, 1093–1102.
- , and B. Fu, 2006: Tropical cyclogenesis associated with Rossby wave energy dispersion of a preexisting typhoon. Part I: Satellite data analyses. *J. Atmos. Sci.*, **63**, 1377–1389.
- , T. F. Hogan, and C.-P. Chang, 2000: Dynamic and thermodynamic regulation of ocean warming. *J. Atmos. Sci.*, **57**, 3353–3365.
- , B. Fu, X. Ge, B. Wang, and M. Peng, 2003: Satellite data analysis and numerical simulation of tropical cyclone formation. *Geophys. Res. Lett.*, **30**, 2122, doi:10.1029/2003GL018556.
- , X. Ge, B. Wang, and Y. Zhu, 2006: Tropical cyclogenesis associated with Rossby wave energy dispersion of a preexisting typhoon. Part II: Numerical simulations. *J. Atmos. Sci.*, **63**, 1390–1409.
- McBride, J. L., and R. Zehr, 1981: Observational analysis of tropical cyclone formation. Part II: Comparison of non-developing versus developing systems. *J. Atmos. Sci.*, **38**, 1132–1151.

- Peng, M. S., J. A. Ridout, and T. F. Hogan, 2004: Recent modifications of the Emanuel convective scheme in the Naval Operational Global Atmospheric Prediction System. *Mon. Wea. Rev.*, **132**, 1254–1268.
- , B. Fu, T. Li, and D. E. Stevens, 2012: Developing versus nondeveloping disturbances for tropical cyclone formation. Part I: North Atlantic. *Mon. Wea. Rev.*, **140**, 1047–1066.
- Ramanathan, V., and W. Collins, 1991: Thermodynamic regulation of ocean warming by cirrus clouds deduced from observations of the 1987 El Niño. *Nature*, **351**, 27–32.
- Ritchie, E. A., and G. J. Holland, 1999: Large-scale patterns associated with tropical cyclogenesis in the western Pacific. *Mon. Wea. Rev.*, **127**, 2027–2043.
- Sun, D.-Z., and Z. Liu, 1996: Dynamic ocean–atmosphere coupling, a thermostat for the Tropics. *Science*, **272**, 1148–1150.
- Tam, C.-Y., and T. Li, 2006: The origin and dispersion characteristics of the observed summertime synoptic-scale waves over the western Pacific. *Mon. Wea. Rev.*, **134**, 1630–1646.
- Wallace, J., 1992: Effect of deep convection on the regulation of tropical sea surface temperature. *Nature*, **357**, 230–231.
- Webster, P. J., and H.-R. Chang, 1988: Equatorial energy accumulation and emanation regions: Impacts of a zonally varying basic state. *J. Atmos. Sci.*, **45**, 803–829.
- Zehr, R. M., 1992: Tropical cyclogenesis in the western North Pacific. NOAA Tech. Rep. NESDIS 61, 181 pp.

Copyright of Monthly Weather Review is the property of American Meteorological Society and its content may not be copied or emailed to multiple sites or posted to a listserv without the copyright holder's express written permission. However, users may print, download, or email articles for individual use.